Fractal fragmentation and small-angle scattering

E M Anitas[1,2]

[1]Joint Institute for Nuclear Research, Dubna 141980, Moscow region, Russia
[2]Horia Hulubei National Institute of Physics and Nuclear Engineering, RO-077125 Bucharest, Romania

E-mail: anitas<at>theor.jinr.ru

Abstract. The small-angle scattering form factor of a three-dimensional idealized fragmentation model based on the concept of renormalization is calculated. The system consists of randomly oriented microscopic fractal objects whose positions are uncorrelated. It is shown that in the fractal region, the monodisperse form factor is characterized by a succession of maxima and minima superimposed on a simple power-law decay, and whose scattering exponent coincide with the fractal dimension of the scatterer. The results could be used to obtain additional structural information about systems obtained through fragmentation processes at microscale.

1. Introduction

Fragmentation processes such as those produced by earth's crust, rocks weathering or explosions, usually lead to to a fractal [1–3] distribution of number of fragments as a function of their sizes over a wide range of scales, and a quantification of these processes using the renormalization group approach has been suggested in [4, 5]. However, an important issue concerns the distribution of fragments at microscales, since they are responsible for the physical properties, such as hydraulic conductivity or moisture characteristics in soils [6].
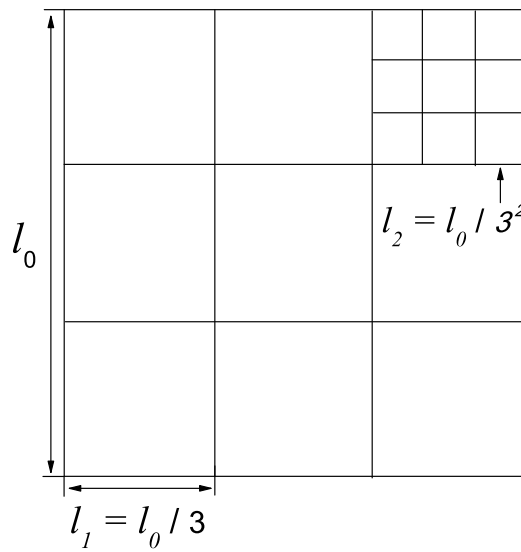
An important technique for investigating the microstructure of various types of systems and which addresses the issue of size distribution, including the smallest and largest components, is small-angle scattering (SAS) [7,8] which yields the differential elastic cross section per unit solid angle as a function of the momentum transfer. This technique has been successfully used in studying the property of self-similarity across nano- and microscales [2], such as various types of elastomeric membranes [9–12], cements [13], semiconductors [14], magnetic [15,16] or biological structures [17–19], and therefore the concept of fractal geometry coupled with SAS technique can give new insights regarding the structural characteristics of such fractal systems [20–27]. One of the main parameters which can be obtained is the fractal dimension D [1]. For a mass fractal it is given by the scattering exponent of the power-law SAS intensity $I(q) \propto q^{-D}$ where $0 < D < 3$.

In this paper, we develop an idealized theoretical model based on renormalization group approach which could describe fragmentation processes, and calculate the mono- and polydisperse form factor. We show how to obtain the fractal dimension, and how to estimate the smallest and largest radius of the fractal from SAS data.

2. Model

We start with a cube of edge length l_0 ($m = 0$; initiator) and in the first iteration ($m = 1$) the number of cubes which are kept is related to the probability f that the initiator will be fragmented into 27 cubes of

Figure 1. A two-dimensional projection of the fragmentation model. The probability that the cube with edge length l_0 ($m = 0$; initiator) will be fragmented into 27 cubes of edge length l_1 is f.

edge length $l_1 = l_0/3$. By calculating the number of fragmented elements and their linear sizes, it can be shown that the fractal dimension is given by [4]:

$$D = 3\frac{\log(27f)}{\log 27},\tag{1}$$

with $1/27 < f < 1$, and thus $0 < D < 3$. Fig. 1 illustrates the construction of a generic model of fragmentation, where the sizes of remaining cubes at m-th iteration is given by $l_m = l_0/3^m$.
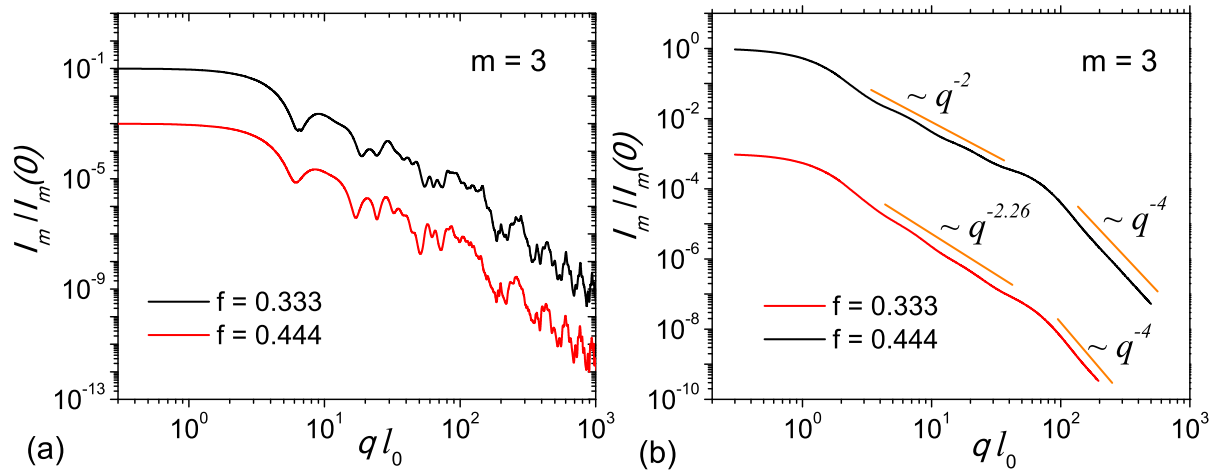
3. Theoretical background on SAS

Here we restrict ourselves to two-phase systems, which are composed from homogeneous units of mass density ρ_m. The units are immersed into a solid matrix of pore density ρ_p. Then [7, 8] we can consider the system as if the units were frozen in a vacuum and had the density $\Delta\rho = \rho_m - \rho_p$. The density $\Delta\rho$ is called scattering contrast, and thus, the scattering intensity is given by

$$I(q) = n|\Delta\rho|^2 V^2 \left\langle |F(\boldsymbol{q})|^2 \right\rangle,\tag{2}$$

where n is the fractal concentration, V the volume of each fractal, and $F(\boldsymbol{q})$ the normalized form factor $F(\boldsymbol{q}) = (1/V)\int_V e^{-i\boldsymbol{q}\cdot\boldsymbol{r}}\mathrm{d}\boldsymbol{r}$, obeying $F(0) = 1$. The brackets $\langle\cdots\rangle$ stand for the ensemble averaging over all orientations of $\boldsymbol{q}$. Once a deterministic fractal is composed of the same objects, say, N cubes of edge length l, then $F(\boldsymbol{q}) = \rho_{\boldsymbol{q}}F_0(ql)/N$, with $\rho_{\boldsymbol{q}} = \sum_j e^{-i\boldsymbol{q}\cdot\boldsymbol{r}_j}$ the Fourier component of the density of the cubes, and $\boldsymbol{r}_j$ are the center-of-mass positions of cubes. Here the cube form factor of unit edge length is given by [7] $F_0(\boldsymbol{t}) = (8/t_x t_y t_z)\sin(t_x/2)\sin(t_y/2)\sin(t_z/2)$. Therefore, the scattering intensity becomes $I(q) = I(0)S(q)|F_0(ql)|^2/N$, with $I(0) = n|\Delta\rho|^2 V^2$ and the structure factor is defined by $S(q) \equiv \langle\rho_{\boldsymbol{q}}\rho_{-\boldsymbol{q}}\rangle/N$.

4. Results and Discussion

The monodisperse form factor at m-th iteration can be written as [23,25] $F_m(\boldsymbol{q}) = F_0(l_m q)\prod_{i=1}^m G_i(\boldsymbol{q})$ with $m = 1, 2, \cdots$ is the generative function of the fractal and it specifies the positions of the scattering

Figure 2. SAS from an idealized fragmentation model for two values of the probability f. a) Monodisperse intensity; b) Polydisperse intensity ($\sigma_r = 0.4$). The curves are shifted vertically for clarity.

cubes inside the fractal. For well-known systems such as Cantor sets or Vicsek fractals $G_i(\boldsymbol{q})$ has known analytical expressions [23, 25]. Thus, the scattering intensity becomes [25]

$$I_m(q)/I_m(0) = \left\langle |F_m(\boldsymbol{q})|^2 \right\rangle. \tag{3}$$

The monodisperse SAS intensity for various values of f is shown in Fig. (2a), where it can be seen that the intensity is characterized by three main regions: a plateau (Guinier region) at low q ($q \lesssim 1/l_0$), an intermediate (fractal) region at $1/l_0 \lesssim q \lesssim 1/l_m$, and a decay proportional to q^{-4} (Porod region) at high q ($1/l_m \lesssim q$). These regions allows us to obtain the size of the generator (from the end of Guinier region), and the smallest size of the scatterers found in the fractal (from the end of the fractal region). In addition, from the Porod region we can extract information about the specific surface of the fractal.

The value of the fractal dimension can be obtained if we take into account the polydispersity of the scatterers. Thus, we consider a distribution function $D_N(l)$ of sizes in such a way that $D_N(l)\mathrm{d}l$ gives the probability of finding a fractal whose size falls within $(l, l + \mathrm{d}l)$. We consider a log-normal distribution, and therefore, the polydisperse SAS intensity is given by [25]

$$I_m(q) = n|\Delta\rho|^2 \int_0^\infty \left\langle |F_m(\boldsymbol{q})|^2 \right\rangle V_m^2 D_N(l)\mathrm{d}l, \tag{4}$$

where V_m is the total volume at the m-th iteration.

Fig. (2b) shows the polydisperse SAS intensity obtained from Fig. (2a) together with Eq. (4). The results clearly show a smoothing of the scattering curves, as expected, and with the scattering exponent in the fractal region, being given by Eq. (1).

5. Conclusion

We have developed a model for describing fragmentation processes based on $3D$ fractal and have used the SAS technique to characterize the microstructural properties of such fragments.

We have calculated the monodisperse and polydisperse SAS intensities, and have shown how to obtain the smallest and largest sizes inside the fractal. We have shown that the slope of SAS intensity coincide with the fractal dimension of the fractal, as given by Eq. (1).

The suggested model can be used in understanding various physical properties such as hydraulic conductivity or moisture characteristics for systems obtained through fragmentation.

References

[1] Mandelbrot B B 1983 *The Fractal Geometry of Nature* (W.H. Freeman)
[2] Gouyet J F 1996 *Physics and Fractal Structures* (Springer)
[3] Vicsek T 1989 *Fractal Growth Phenomena* (Singapore: World Scientific)
[4] Turcotte D L 1986 *Journal of Geophysical Research* **91** 1921–1926
[5] Turcotte D L 1997 *Fractals and Chaos in Geology and Geophysics* (Cambridge University Press)
[6] Bittelli M, Campbell G S and Flury M 1999 *Soil Sci. Soc. Am. J.* **63** 782–788
[7] Glatter O and Kratky O 1982 *Small-angle X-ray Scattering* (London: Academic Press)
[8] Feigin L A and Svergun D I 1987 *Structure Analysis by Small-Angle X-Ray and Neutron Scattering* (NY: Plenum press)
[9] Balasoiu M, Anitas E M, Bica I, Erhan R, Osipov V A, Orelovich O L, Savu D, Savu S and Kuklin A I et al 2008 *Optoelectronics and Advanced Materials - Rapid Communications* **2** 730–734
[10] Balasoiu M, Craus M L, Kuklin A I, Plestil J, Garamus V, Islamov A K, Erhan R, Anitas E M, Lozovan M, Tripadus V, Petrescu C, Savu D, Savu S and Bica I 2008 *Journal of Optoelectronics and Advanced Materials* **10(11)** 2932–2936
[11] Anitas E M, Balasoiu M, Bica I, Osipov V A and Kuklin A I 2009 *Optoelectronics and Advanced Materials - Rapid Communications* **3** 621–624
[12] Balasoiu M, Craus M L, Anitas E M, Bica I, Plestil J and Kuklin A I 2010 *Physics of the Solid State* **52(5)** 917–921
[13] Das A, Mazumder S, Sen D, Yalmali V, Shah J G, Ghosh A, Sahu A K and Wattal P K 2014 *J. Appl. Cryst.* **47** 421–429
[14] Cho K, Biswas P and Fraundorf P 2014 *J. Ind. Eng. Chem.* **20** 558
[15] Craus M L, Islamov A K, Anitas E M, Cornei N and Luca D 2014 *Journal of Alloys and Compounds* **592** 121–126
[16] Naito T et al 2014 *Eur. Phys. J. B* **86** 410
[17] Yadav I, Kumar S, Aswal V K and Kohlbrecher J 2014 *Phys. Rev. E* **89** 032304–1
[18] Gebhardt R 2014 *J. Appl. Cryst.* **47** 29–34
[19] Maji J, Bhattacharjee S M, Seno F and Trovato A 2014 *Phys. Rev. E* **89** 012121
[20] Schmidt P W and Dacai X 1986 *Phys. Rev. A* **33** 560–566
[21] Martin J E and Hurd A J 1987 *J. of Appl. Cryst.* **20** 61–78
[22] Schmidt P W 1991 *J. of Appl. Cryst.* **24** 414–435
[23] Cherny A Y, Anitas E M, Kuklin A I, Balasoiu M and Osipov V A 2010 *J. Appl. Cryst.* **43** 790–797
[24] Cherny A Y, Anitas E M, Kuklin A I, Balasoiu M and Osipov V A 2010 *J. Surf. Invest.* **4** 903–907
[25] Cherny A Y, Anitas E M, Kuklin A I and Osipov V A 2011 *Phys. Rev. E* **84** 036203–1–036203–11
[26] Cherny A Y, Anitas E M, Osipov V A and Kuklin A I 2014 *J. Appl. Cryst.* **47** 198–206
[27] Anitas E M 2014 *Eur. Phys. J. B* **87** 139